The influence of the initial near-surface microstructure and imposed stress level on the running-in characteristics of lubricated steel contacts

Angelika Brink, Klaudia Lichtenberg,* and Matthias Scherge†
Fraunhofer IWM, MikroTribologie Centrum μTC, Rintheimer Querallee 3, 76131 Karlsruhe
(Dated: April 13, 2016)

The tribological behavior of polished and lapped 56NiMoCrV7 and Ck45 disks with lubrication was studied to link the impact of initial near-surface microstructure to the running-in behavior of the systems. The tests were performed using a pin-on-disk tribometer with radionuclide technique to resolve ultra-low wear rates. For the running-in different stressing regimes were applied. Whereas the lapped disks developed low friction and wear as response to a high-power running-in, the polished disks had to be stressed by a step-wise increase in load to achieve a similar result. In addition, the duration of some load steps and the sliding velocity had to be adjusted in order to obtain a proper running-in. With the help of focused ion beam and transmission electron microscopy the response of the microstructure to the stressing conditions was investigated. It turned out that the quality of the running-in crucially depends on a subtle equilibrium between material strengthening and softening. Strengthening by finishing and running-in was a prerequisite for the formation of the third body, whereas softening resulted in scuffing. When it was possible to charge the near-surface material in relation to its strengthening capabilities, low wear rates in the nanometer per hour regime were obtained.

I. INTRODUCTION

Besides the action of oil and additives, the way a tribological system performs crucially depends on the type of surface finish [1] and the first minutes of operation, that means the running-in [2]. During the running-in, first the topographies adjust (topographical running-in), then the deposited energy results in heat, plastic deformation and intermixing as well as material deposition. The involved friction bodies respond by changes in topography (dissipative structures [3], material transfer or film formation), changed near-surface microstructure and modified chemical composition. Godet called this the third body formation [4]. The introduction of heat was discussed by Kuhlmann-Wilsdorf and others [5, 6]. Targeting the materials response, Rigney et al. investigated the involved mechanism leading to changes in near-surface structure and to the introduction of foreign elements as result of intermixing processes [3, 7–9]. Martin et al. elucidated on film formation effects due to tribo-chemical reactions with oils containing ZDDP [10]. The general consensus is that friction and wear are significantly influenced by interfacial processes as well as mechanical and chemical properties of the near-surface material. Plastic deformation, flow of asperities and micro-crackings are the most prominent mechanisms [4]. Despite all research, the tribological impact of the evolving third body on low friction coefficients and small wear rates is still a matter of discussion. Moreover, it is not clear why only under specific conditions the system can develop low friction coefficient and small wear rate and what the predominant influencing parameters are.

In the past, influencing parameters like the total dissipated power during running-in or the sequence of operation points (contact pressures and sliding velocities) were discussed. Systems that were subjected to a high-power running-in developed significantly lower friction than systems operated under low initial loadings [11]. In addition to lower friction, the high-power running-in yielded lower wear rates after a shorter running-in time. The results suggest that the initial power of friction $\mu F_{\mathrm{n}} v$ influences the long-term behavior of the entire system as described in [12]. Volz discovered that differently designed running-in routines, with a certain sequence of pressures and velocities, result in different friction and wear patterns [13]. His findings were based on engine bench tests using high-resolution and continuous wear measurements with radionuclide technique (RNT) [14]. At this time the first attempts were undertaken to design running-in routines. The success, however, was limited since the formation of the third body was not considered. Meanwhile, this issue was pursued over the last 15 years and a tremendous progress can be witnessed in research on tribological systems showing ultra-low wear rates.

The aim of this study is to show how initial conditions set by the microstructure and the way how contact pressure and sliding velocity are controlled lead to the development of lowest coefficients of friction and ultra-low wear rates as desired for lubricated tribological contacts. The role of surface finishing – polishing and lapping – was evaluated with focus on initial microstructural properties. To reduce complexity, radionuclide-assisted pin-on-disk tribometry was carried out. Since steel is widely used in mechanical engineering, lubricated steel-steel contacts were evaluated. Whereas the pin material was kept constant, the material of the disks differed in hardness. By means of focused ion beam analysis (FIB) and transmission electron microscopy (TEM) the near-surface volume was characterized prior and after the tri-

* present address: Karlsruher Institute of Technology KIT, IAM-Werkstoffkunde, Kaiserstraße 12, 76131 Karlsruhe
† corresponding author: matthias.scherge@iwm.fraunhofer.de

bological tests to monitor the evolution of the microstructure. Photoelectron spectroscopy (XPS) was applied to follow the chemical changes due to shear. Nanoindentation was used to characterize the mechanical properties of the near-surface material. As a first order approximation, nanoindentation hardness was considered a measure of conditioning, since by changing grain-size and dislocation density, the micro-hardness is affected.

II. EXPERIMENTS

Pin-on-disk tribometer tests were performed on steel disks made of 56NiCrMoV7 (disk D1) and Ck45 (disk D2), using a pin made of C86 carbon steel. 56NiCrMoV7 is an alloyed steel with following chemical constituents (at%): C: 0.5-0.6; Si: 0.1-0.4; Mn: 0.65-0.95; P: <0.03, S: <0.03; Cr: 0.1-1.2; Ni: 1.5-1.8; Mo: 0.45-0.55; V: 0.07-0.12. Ck45 (= AISI/SAE 1045) is a plain carbon steel with following chemical constituents (at%): C: 0.43-0.5; Si: <0.4; Mn: <0.5; S: <0.035; Cr+Ni+Mo: <0.65. 56NiCrMoV7 exhibits a homogeneous microstructure with less than 2% of residual austenite and minor carbidic precipitates at the grain boundaries. 56NiCrMoV7 has a martensitic microstructure, whereas Ck45 and C86 have a ferritic/perlitic microstructure. The pin C86 (= AIS/SAE 1086) contains the following chemical constituents (at%): C: 0.35-1; Si: 0.1-0.3; Mn: 0.5-1.2; P: <0.035; S: <0.035; Cu: <0.2. The steel disks were cut, ground and annealed. After annealing, half of the disks was lapped with a 9 µm suspension at a working pressure of some MPa. The other half was handpolished with cloth and suspension (grain size ≈ 1 µm) at a working pressure of less than 1 MPa. The polishing procedure was applied to the pins as well, see Tab. I. The materials selection was a compromise between simplicity, applicability in mechanical engineering and further use of the results to feed atomistic simulations (to be published).

TABLE I. Samples, compositions, Vickers hardness, heat treatment temperature and roughness.

	D1	D2	pin
material	56NiCrMoV7	Ck45	C86
HV01 lapped and polished[1]	400±20	270±20	450±20
austenitizing temperature	850°C	880°C	N/A
annealing temperature	630°C	530°C	N/A
R_a [2] polished	12 nm	10 nm	10 nm
R_a [2] lapped	150 nm	200 nm	N/A

[1] Microhardness Vickerstest with Wolpert VDT 12 using DIN EN ISO 6507 - 1:2006, test method HV, load duration 10 s

[2] Sensofar-Tech S.L.

Cross sectional secondary electron microscopy (SEM) imaging of the new samples was carried out and is presented for D1 after polishing and lapping, see Fig. 1. The polishing procedure did not have a significant influence on the near-surface structure, while lapping introduced clear changes in the near-surface microstructure up to a depth of 2.5 µm. Chemical analysis by XPS revealed that there is no distinct difference between the polishing and lapping process, see Fig. 2. The penetration depths of O and C/CH_x for both procedures ranged between 10 nm and 20 nm. The shift to larger penetration depths after lapping can be related to increased roughness. The depth profiles for D2 and pin were similar, not shown here. In contrast, topography and macroscopic hardness of the polished and lapped disks showed distinct differences, see Tab. I. The relation between disk and pin hardness was about 1 for D1 and about 0.5 for D2. Microscale hardness measured by nanoindentation showed higher values for the lapped modification of D1 as well as for D2 due to a grain refined near-surface layer, see Fig. 3. The difference in hardness between polishing and lapping was more pronounced for steel D1. In addition, the lapped surface showed an increase in roughness. This leads to differences in real contact area between the different disks and the pin.

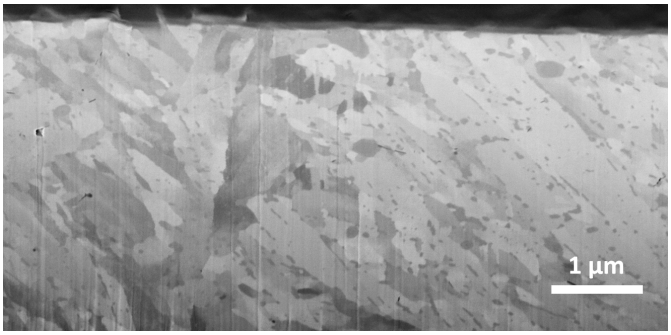

(a)Initial microstructure polished.

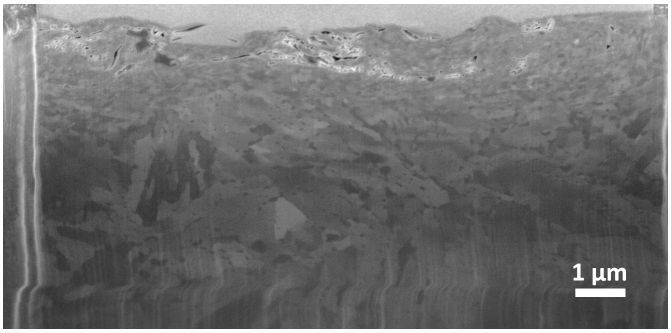

(b)Initial microstructure lapped.

FIG. 1. SEM characterization of FIB cross sections of the initial state of D1 in polished and lapped condition.

The tests with a commercially available pin-on-disk tribometer (BASALT SSD from TETRA GmbH) were carried out with a polyalphaolefine base oil with a dynamic viscosity of 25.7 mPas at a temperature of 50°C. The oil

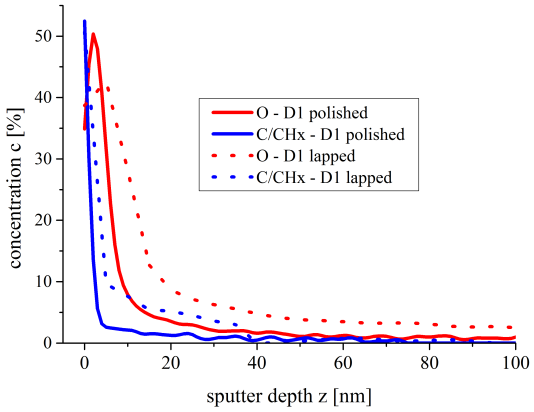

FIG. 2. Chemical depth profile (XPS) of initial the near-surface layer due to lapping and polishing of D1.

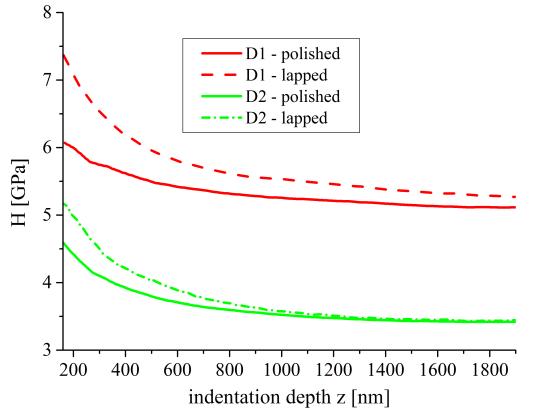

FIG. 3. Microscale hardness depth profile of initial near-surface layer of lapped and polished condition of D1 and D2. 50 indents were placed in depth controlled mode. A value was taken every 0.2 s.

was free of additives, thus, tribochemical reactions other than with carbon and hydrogen can be excluded. The oil circuit was filled with 2.5 liters. Using a central nozzle, oil was directly supplied to the disk and spread due to rotation. From the oil sump underneath the disk, a pump sucks the oil into the RNT sensor assembly and brings it back to the disk via the nozzle. The disks have a diameter of 75 mm and faced a flat C86 pin. The pins have a diameter of 5 mm with a slightly tapered edge to prevent undesired cutting into the disk. To achieve a flat contact between pin and disk, the pin holder allowed a self-regulating adjustment. The tribometer covers a wide range of normal forces between 10 N and 1,000 N and sliding velocities between 0.1 m/s and 10 m/s.

To achieve a sufficiently good running-in, the tests were carried out at a constant normal force of 400 N, which corresponds to a Hertzian pressure of 20 MPa, at 0.1 m/s sliding velocity. This parameter set was chosen because pre-tests with a lapped steel disk using continuous friction and wear recordings indicated a stable running-in behavior for these conditions. This kind of running-in is called a high-power running-in since even a small further increase in loading resulted in a failure of the system. Friction and wear of the pin were monitored continuously by radionuclide technique (RNT). In the entire pin area facing the disk nuclidic wear markers were generated. Across the pin the simultaneous contact of many asperities contributes to wear. Thus, the amount of wear is an average of all microscopic wear events. Although only the pin was irradiated for the RNT, conclusions about the wear behavior of the entire system can be drawn. In addition, the disk wear tracks were quantified after the test by white light interferometry, giving a wear area in μm^2. With the radionuclide technique micrograms of wear can be detected in the oil circuit which corresponds to a wear rate of a few nanometers per hour. Details of the method were described by Scherge et al. [14]. To obtain wear tracers, pins were subjected to low-energy neutron radiation. Cr-51 was used as nuclide. The oil circuit of the tribometer was connected to a gamma detector (Zyklotron AG) allowing continuous monitoring of wear in the oil. To account for decay effects, a reference measuring device was included in the oil circulation.

III. RESULTS

A. Friction and Wear behavior

In order to qualify a tribological system with respect to its running-in behavior, a definition becomes necessary: A proper running-in is achieved when the tribological systems quickly develops low friction and small wear rate at high system stability and low sensitivity. Stability refers to the effect that the system quickly passes the running-in and adopts a constant wear rate. Tribological systems can have several stable states. Sensitivity reflects the property of the system that friction and wear show negligible response to changes of the boundary conditions such as oil temperature, load or speed changes. The polished and the lapped disks exhibited a distinctively different running-in behavior. While the polished disks of both steels seized already during the initiation of the experiment, i.e., during the load increase up to 400 N, the lapped samples could be charged directly with 400 N without failure. The polished disks failed by scuffing following the definition of Fenske et al. [15]. This definition is equal to the ASTM standard definition for scuffing. All measurements presented in the following sections were repeated 3 times.

1. *Running-in performance of D1*

When disk D1 lapped was subjected to the high-power running-in, friction showed a very short topographical running-in followed by a few fluctuations but quickly developed stable and low coefficients, see Fig. 4.

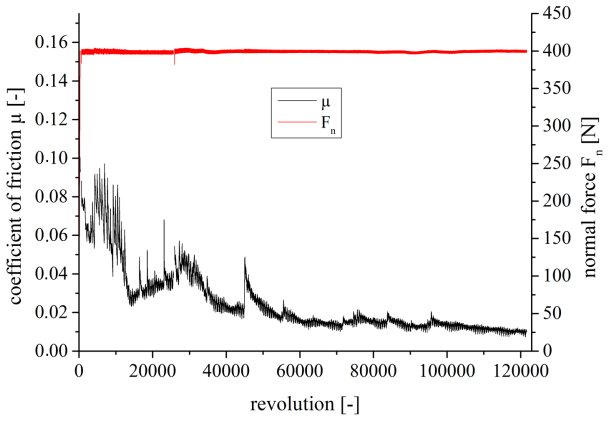

FIG. 4. Running-in at 400 N and 0.1 m/s of D1 lapped. 120,000 revolutions correspond to a sliding distance of 18 km.

To obtain a similar result for D1 polished, the high-power running-in had to be replaced by step-wise increase in normal force from 25 N to 400 N, see Fig. 5. This kind of running-in program was composed empirically. As of today no straight forward procedure for the generation of a successful running-in procedure exists. The first 4 steps in load caused sudden jumps of the coefficient of friction to higher values followed by a decrease to the initial friction level. Beginning with the fifths increase in load (250 N) the running-in became stable and showed a strong resemblance to the behavior of D1 lapped. At the end of the experiments the coefficients of friction of D1 polished and D1 lapped were almost equal. In terms of pin wear, system D1 polished showed wear rates on the order of 3 nm/h, whereas D1 lapped showed negligible wear. The wear loss of both disks was comparably low and ranged between 150 µm^2 and 200 µm^2.

2. *Running-in performance of D2*

The lapped modification of D2 revealed no difference in the running-in behavior compared with the lapped modification of D1. As for D1 lapped, D2 lapped was able to tolerate the initial fast increase in loading. The wear rate of the pin was less than 2 nm/h. The wear loss of the disk was approximately 500 µm^2, i.e. higher than for D1 lapped. The load steps used for D1 polished were applied to D2 polished as well. After a considerable number of failed experiments, i.e., instant scuffings, a successful running-in was found for a sequence of loads

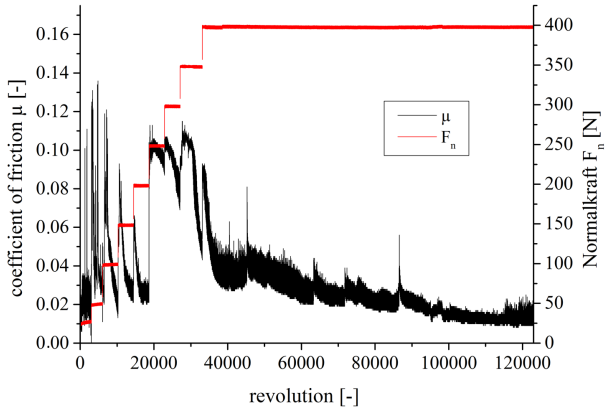

FIG. 5. Running-in at 0.1 m/s and a step-wise increase in load of D1 polished. 120,000 revolutions correspond to a sliding distance of 18 km.

as shown in Fig. 6. The velocity had to be increased to $v = 0.2$ m/s and the load step of 150 N had to be extended. After passing all further load steps, friction became as low as for D1 polished. However, the running-in showed increased sensitivity to load steps compared with D1 polished and the repeatability of the experiments became poorer. In addition, the pin showed a wear rate of 1,300 nm/h already for the second load step of 50 N. The wear loss of the disk (4,000 µm^2) was considerably higher than the wear loss of D1 polished.

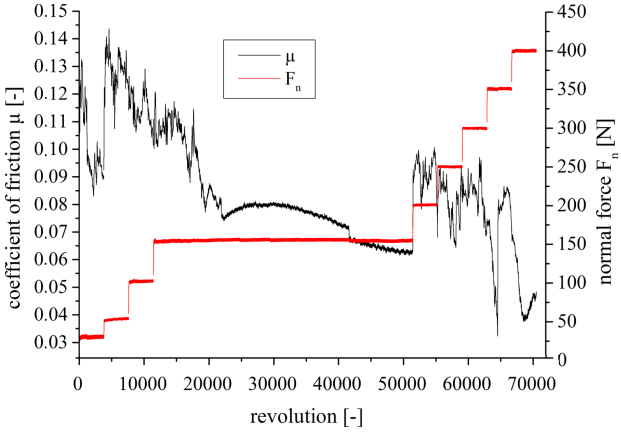

FIG. 6. Running-in with v =0.2 m/s for D2 polished. 70,000 revolutions correspond to a sliding distance of 10.5 km.

B. Microstructural Analysis

In order to observe changes in microstructure caused by the different running-in procedures, cross sections with focused ion beam were prepared. The SEM im-

ages of the D1 cross sections are shown in Fig. 7. The cross sections were placed in sliding direction. The differences in near-surface microstructure of D1 polished and D1 lapped compared with the state of the bulk are obvious. Both conditions, lapped and polished, developed a similar nanocrystalline layer, indicated by arrows in Figs. 7a) and b). Both D1 polished and D1 lapped showed a grain refined structure compared to the initial state, see Fig. 1a). The grains are deformed in sliding direction and have a longitudinal grain shape. The curve-fit in the image indicates the displacement with respect to a perpendicular to the surface and specifies the depth of deformation. In Fig. 7c) a TEM image and associated diffraction pattern of the encircled area are shown, revealing grain sizes in the range of 10 nm. The microstructure of D2 lapped was very similar to that of D1 lapped. In contrast, due to high wear, D2 polished showed no signs of grain size reduction.

For D1 polished additional cross sections were taken during the load step running-in after 25 N and 150 N to characterize the progress in microstructural evolution, see Fig. 8. Already after the very first load step of 25 N, a distinctive grain-refinement was obtained. For further load steps the depth of deformation did not change significantly. After the load step of 150 N the grains in the first 200 nm became orientated parallel to the surface, indicated by the upper dashed line. In addition, a small nanocrystalline layer, marked with arrows in Fig. 8c), was formed. This layer was in the range of 20 nm and not evenly distributed, whereas for 400 N the layer was up to 200 nm thick. We assume that due to the same appearance, compared with the layer after 400 N, that this layer consists of nanocrystalline grains. It became obvious that a normal load increase did not extend the deformation zone into the material, but influenced the near-surface layer with respect to its nanocrystalline structure. A differentiation between the strengthened and nanocrystalline area has to be made here. The strengthened area indeed does not increase with increasing load, the nanocrystalline layer does. In addition, the friction power density decreases by a factor of 10 during the running-in. Deformation mainly acts on the nanocrystalline layer.

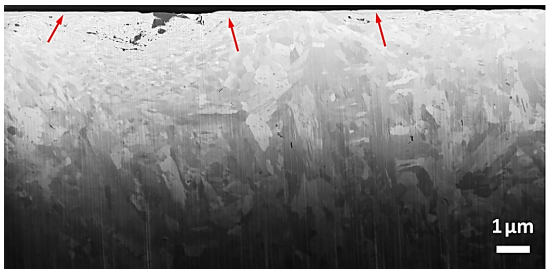

(a)Cross section of D1 lapped after the high-power running-in at 400 N.

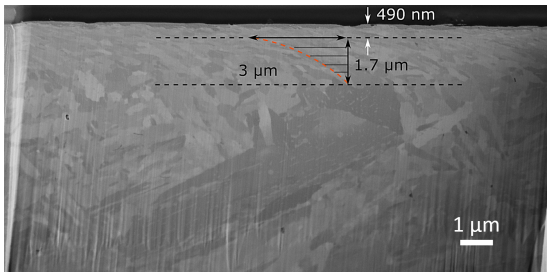

(b)Cross section of D1 polished after passing the load steps up to 400 N.

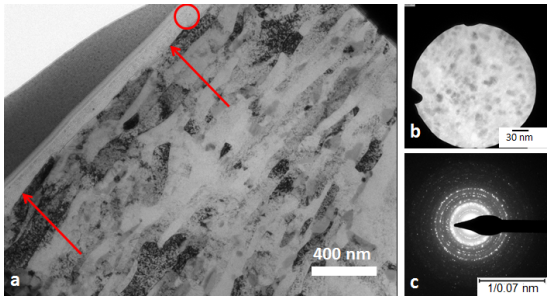

(c)Nanocrystalline layer of D1 polished after passing the load steps up to 400 N.

FIG. 7. a) and b) SEM images of FIB cross sections for D1 polished and D1 lapped for v =0.1 m/s. Sliding direction is from right to left. c) TEM image and diffraction pattern of nanocrystalline layer (red circle).

C. Chemical Analysis

Chemical depth profiles to quantify shear-induced mechanical intermixing were recorded for oxygen, bonded as Fe_2O_3 and for carbon bonded in carbon-hydrogen chains. Other elements revealed no modification due to tribological interaction or the finishing process. The oxygen depth distribution after running-in showed distinct differences between the lapped and the polished initial condition, whereas there is no difference between different materials. The total depth of the oxygen intake was similar for all experiments. The lapped samples of D1 and D2 revealed a smaller oxygen peak than the polished samples, see Fig. 9. The differences in the carbon content represented as C/CHx were not significant.

IV. DISCUSSION

During running-in a significant fraction of the power of friction is transformed into heat. Another fraction generates wear and a third fraction changes the material by plastic flow and intermixing with respect to topography, chemical composition and microstructure. This is the third body formation. For materials with comparable hardness the third body is symmetric. When the hardness of first and second body deviates, the third body can be asymmetric. With respect to the inner structure of the third body the chemical depth profiles reflect the

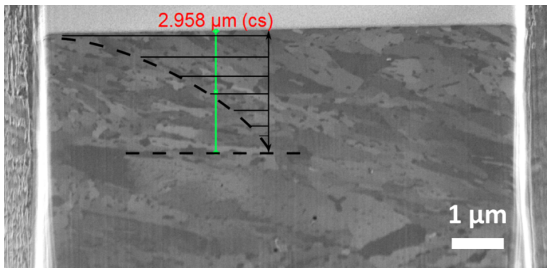

(a)Cross section of D1 polished after passing the load step of 25 N.

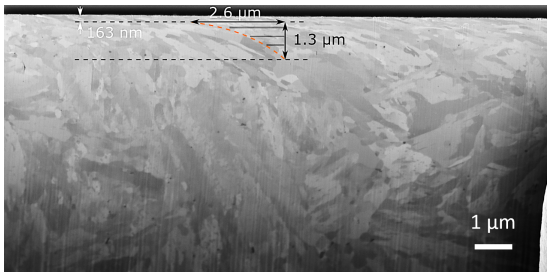

(b)Cross section of D1 polished after passing the load step of 150 N.

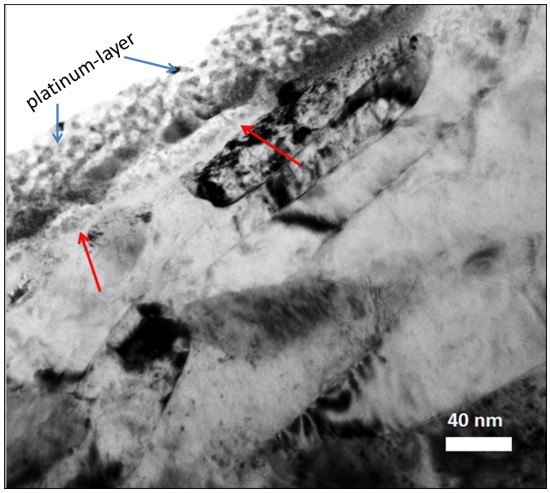

(c)TEM image of D1 polished after passing the load step of 150 N.

FIG. 8. a) and b) SEM images of FIB cross sections for D1 polished after the load step of 25 N and 150 N for $v = 0.1$ m/s. c) TEM image of D1 polished with a running-in stopped after 150 N.

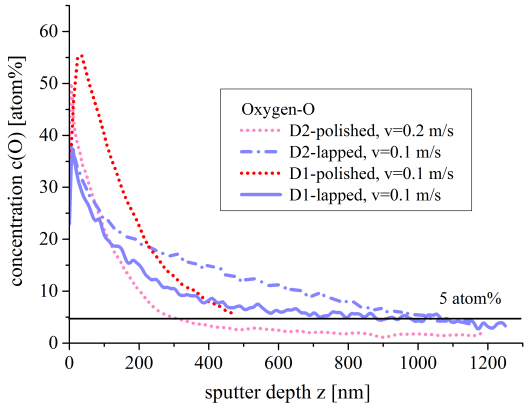

FIG. 9. XPS analysis after running-in for D1 and D2 polished and lapped.

impact of shear, whereas microstructural analysis characterizes the effect of contact pressure and cyclic creep [16]. The third body is the prerequisite for ultra-low wear rates and small coefficients of friction.

In [12] we elucidated on the mechanisms that support a tribological system to develop the third body. The bottom line was that the amount of friction power density at the beginning of the running-in is of crucial importance to the achievement of the superb tribological properties mentioned above. Initial overstressing as well as understressing are detrimental, since too much power density leads to a wear rate that prevents the third body from growing. Understressing, on the other hand, results in a situation that does not provide enough power to ignite the necessary mechano-chemical reactions to form the third body. Only an appropriate amount of power can bring the system into the desired running-in corridor by inducing the right degree of plastic flow, mechanical intermixing and mechano-chemical reactions. For some material systems the running-in corridor is wide, this means a large variety of initial stressing conditions induce a proper running-in. For other systems the corridor can be narrow, thus subtle changes in initial conditions decide about success or failure.

At the beginning of third body formation the metal has to be locally charged above its yield strength to deform the material lateraly homogeneous as reported by Rogers [17]. Czichos described localized stress enhancements as important for the initiation of plastic flow and rendered the rising temperature in the contact area as crucial for the performance of a tribological system [18]. When the material received a pre-strenghtening due to finishing, temperature can increase further. This temperature increase, also known as flash temperature, promotes the third body formation and decreases friction and wear as well as adhesion [19]. However, when the initial stressing is too intense, softening due to elevated flash temperatures can exceed strengthening. Then the plastic deformation process becomes instable and the homogeneity of plastic deformation suddenly changes to localized severe deformation. This kind of instability associated with severe plastic work and further intensified heat generation elapses in a very short time. The process can be considered adiabatic [17]. Fenske et al. observed softening of steel and the formation of retained austenite right before the scuffing failure and considered the scuffing-mechanism an adiabatic shear plastic instability

[15].

Since scuffing involves rearrangements of deeper regions, the mechanical stability of the bulk plays a significant role. Therefore, the analysis of wear mechanisms at the transition from ultra-low wear to severe wear – this means at the left and right edge of the runnig-in corridor – must consider microscopic near-surface properties as well as macroscale effects like hardness of both materials. In addition, mechanical conditioning of the tribological system – here polishing and lapping – plays an important role. Whereas the conditioning due to polishing was nearly negligeable, lapping imposed a significant influence. Based on these model perceptions the discussion focuses on the following questions:

- Why was it possible to perform a high-power running for D1 and D2 lapped?
- What caused scuffing of D1 and D2 polished?
- What happened during the load step running-in of D1 and D2 polished?

A. Why was it possible to perform a high-power running for D1 and D2 lapped?

Before proceeding with a detailed discussion it has to be pointed out that identifying the appropriate stressing conditions making up the high-power running-in for D1 and D2 lapped was not a straightforward process following an existing recipe. On the contrary, running-in conditions had to be identified iteratively. First Stribeck curves with numerous operation points were run and friction and wear were recorded continously. The response of the system, e.g. significant changes in friction and wear rate after certain stressing steps, pointed at key running-in loads and velocities. The appropriate loading conditions comprised a single, but high normal force of 400 N and a constant sliding velocity of 0.1 m/s. As a result, both systems where brought into the running-in corridor and developed the third body. In addition to the energetic control of the running-in, the capability of the system to perform a running-in was increased by sample finishing. Due to lapping the initial grain sizes of D1 and D2 were significantly reduced. According to the Hall-Petch relation a decreased grain size results in increased strengthening, since the increased number of grain boundaries as well as the piled up dislocations hinder the flow of material due to shear stress. The XPS depth profiles, showing element concentrations originating from plastic flow and intermixing, indicated that shear was located close to the surface, see Fig. 9. Additionally, lapping generated a wave-like roughness of the disk surfaces, see Fig. 1. Roughness is a measure of the real contact area and controls the friction power density, since shear is mainly localized at the summits of the asperities. Both, the strengthening effect due to homogeneous plastic deformation and the localization of friction power density support the formation of the third body as described above.

B. What caused scuffing of D1 and D2 polished?

Due to low roughness the tribological response of the systems became erratic and was either completely hydrodynamic with lowest coefficients of friction or within boundary lubrication. Therefore, the system failure involved the sudden breakdown of the lubricating film and the near-surface oxide [20]. Both solid surfaces instantly contacted and scuffed. Dyson et al. [21] described the mechanism of scuffing-failure in an engineering way as "gross damage characterized by the formation of local welds between the sliding surfaces", not to be mixed up with seizure, where the system stops running. There are several descriptions for this failure mechanism in literature and the phenomenology is described in quite different ways. Ludema [22] reported on roughening of surfaces due to transfer of material in both directions with and without material loss. Fenske et al. [15] extended this model and gave a more generalized overview on the scuffing-mechanism. The total system damage was considered a sudden increase of the coefficient of friction, contact temperature and vibration. As a result, the surface roughness increases due to a significant increase in plastic flow.

The observations for D1 and D2 polished underlined that charging the systems with a normal force higher than 40 N caused the same failure mechanism as described by Ludema [22] and Dyson [21], see Fig. 4. Since the polished samples have a lower microhardness – 25% for D1 and 15% for D2 – and insufficient strengthening, compared to the lapped ones, see Fig. 3, we assume that shear can not be transformed into homogeneous, that means lateraly evenly distributed, plastic deformation. The small deviations in roughness connected to a slightly different initial contact situation might contribute to this behavior. However, all figures showing coefficients of friction as function of time underline that topographical adjustments were just a matter of a few revolutions. As a consequence, the instability described above occurs and the system fails. Systems D1 and D2 have a very narrow running-in corridor. The chosen initial conditions caused overstressing, meaning that the system was operated right of the running-in corridor.

C. What happened during the load step running-in of D1 and D2 polished?

Since the initial mechanical properties of the systems did not allow a high-power running-in, load steps were necessary to pre-strengthen the near-surface material for a further increase in normal force, without inducing inhomogeneous deformation. This can be seen in Fig. 8a). The FIB cross section after the initial load-step of 25 N

showed a grain refined near-surface. Shear force has to be always in a balance with the mechanical properties of the materials, so that homogeneous plastic deformation and intermixing can occur to form the third body in a step-wise manner. As mentioned by Rigney, overcoming of adhesion is an important factor for the evolving of a nanocrystalline layer [8]. Nanocrystalline zones were observed already after the load step of 150 N and revealed an increase in size for increasing normal forces, see Fig. 8b). System D2 apparently was operated at the frontier between ultra-low wear and severe wear, this means at the right edge of the running-in corridor. In this particular range third body formation ceases and mechanisms known as abrasion [23] or tribo-oxidation [24, 25] start to dominate. The system grows instable, shows increased scatter of the coefficient of friction and fails due to excessively high wear. The process of grain structure evolution is affected by the relation between pin and disk hardness. Whereas disk D1 showed comparable hardness, disk D2 was significantly softer. As a result, disk D2 had to be operated at higher sliding velocity to increase the lubricant film thickness, thereby decreasing the friction power density. In addition, the load step of 150 N was extended to give the system time to adjust to the loading level. Despite all adjustments and the low coefficient of friction at the end of the experiment, disk D2 polished failed due to high wear, since the material fatigued.

V. SUMMARY AND CONCLUSIONS

In this work the significant influence of the initial near-surface structure on the running-in behavior was pointed out. In the process of tribological stressing a subtle equilibrium between softening and strengthening is important for the quality of the running-in. The initial near-surface structure can be controlled over a wide range by metal working, especially by finishing [1]. In this work the influence of lubricant additives was not considered. Thus, tribo-chemical reactions did not contribute to the running-in. When the lubricant is additivated, these reactions have to be analyzed as well.

The following conclusions can be drawn:

1. When by conditioning the near-surface material was furnished with the adequate microhardness, a high-power running-in was able to quickly induce low friction and wear. To characterize the mechanical properties of the near-surface material, nanoindentation can be used. When the system has not experienced a sufficient conditioning before tribological stressing, load has to be applied step-wise in order to resume the conditioning during operation.

2. The macrohardness ratio comes into play when plastic deformation processes possess subordinate influence. By adjusting the stressing sequence of the running-in, the tribological systems can be tuned towards low coefficients of friction and low wear rates rendering test field design a powerful lever of tribological optimization. For the material couple with the same macrohardness of pin and disk, it was possible to condition the near-surface by a step-wise increase in load. This procedure was not successful for the system having a large difference between disk and pin hardness.

3. To perform a high-power running-in, the system has to be monitored by continuous and high resolution friction and wear measurement to prevent overstressing.

4. The findings can be applied to ductile materials with the ability of strengthening. However, other mechanisms have to be taken in account for materials with high precipitation density.

ACKNOWLEDGMENTS

We gratefully acknowledge the Robert Bosch GmbH and Daimler AG for their financial support of this work. The author would also like to thank Patrice Brenner and Dominic Linsler for their support with the focused ion beam microscopy.

[1] P. Berlet, M. Dienwiebel, and M. Scherge, "The effect of sample finishing on the tribology of metal/metal lubricated contacts," Wear, 268 (11-12) (2010), 1518-1523 pp.

[2] P. J. Blau, "Running-in: Art or Engineering?" J. Materials Engineering 13 (1) (1991), 47-53 pp.

[3] M. Scherge, D. Shakhvorostov, and K. Pöhlmann, "Fundamental wear mechanism of metals," Wear, 255 (2003), 395-400 pp.

[4] M. Godet, "The third-body approach: A mechanical view of wear," Wear 100 (1984), 437-452 pp.

[5] D. Kuhlmann-Wilsdorf, D. Makel, and N. Sondergaard, "Refinement of Flash Temperature Calculations (Proc. Conf.) F.A. Schmidt, P.J. Blau (Eds.)," Engineered Materials for Advanced Friction and Wear Applications (1988), 23-32 pp.

[6] H. Blok, "Theoretical study of temperature rise at surfaces of actual contact under oiliness lubricating conditions," Proc. Gen. Discuss. Lubr., 2 (1937), 222-235 pp.

[7] D. A. Rigney and S. Karthikeyan, "The evolution of tribomaterial during sliding: A brief introduction," Trib. Letters, 39 (2000), 3-7 pp.

[8] D. Rigney, "Transfer, mixing and associated chemical and mechanical processes during the sliding of ductile materials," Wear, 245 (2000), 1-9 pp.

[9] A. Fischer, "Subsurface microstructural alterations during sliding wear of biomedical metals. modelling and experimental results," Comp. Mat. Sc., 46 (2009), 586-590 pp.

[10] J. Martin, "Antiwear Mechanisms of Zinc Dithiophosphate: A Chemical Hardness Approach," Trib. Let, 6 (1999), 1-8 pp.

[11] D. Shakhvorostov, K. Pöhlmann, and M. Scherge, "Structure and mechanical properties of tribologically induced nanolayers," Wear, 260 (2006), 433-437 pp.

[12] M. Scherge, D. Linsler, and T. Schlarb, "The running-in corridor of lubricated metalmetal contacts," Wear (2015), 60-64 pp.

[13] J. Volz, *Erstellung optimaler Einlaufprogramme von Dieselmotoren (Optimized running-in routines for diesel engines*, Phd-thesis, University of Karlsruhe (1976).

[14] M. Scherge, K. Pöhlmann, and A. Gervé, "Wear measurement using radionuclide-technique (RNT)," Wear, 254 (2003), 801-817 pp.

[15] O. Ajayi, J. Hersberger, J. Zhang, H.Yoon, and G. Fenske, "Microstructural evolution during scuffing of hardened 4340 steel - implication for scuffing mechanism," Tribology International, 38 (2005), 277-282 pp.

[16] A. Fischer, S. Weiss, and M. Wimmer, "The tribological difference between biomedical steels and CoCrMo-alloys," Journal of the Mechanical Behavior of Biomedical Materials (2012), 50-62 pp.

[17] H. Rogers, "Adiabatic plastic deformation," Ann. Rev. Mater. Sci., 9 (1979), 283-311 pp.

[18] H. Czichos, *Tribology: a system approach to the science and technology of friction, lubrication and wear* (Elsevier Science, 1978).

[19] L. Chen and D. Rigney, "Adhesion theories of transfer and wear during sliding of metals," Wear (1990), 223-235 pp.

[20] D. Dowson, "Elastohydrodynamic and micro-elastohydrodynamic lubrication," Wear, 190 (1995), 125-138 pp.

[21] A. Dyson, "Scuffing - a review," Tribology International, 8 (1975), 77-87 pp.

[22] K. Ludema, "A review of scuffing and running-in of lubricated surfaces with asperities and oxides in perspective." Wear, 100 (1984), 315-331 pp.

[23] K.-H. Z. Gahr, *Microstructure and wear of materials* (Elsevier Verlag, 1987).

[24] T. Quinn, D. Rowson, and J. Sullivan, "Application of the oxidational theory of mild wear to the sliding wear of low alloy steel," Wear, 65 (1980), 1-20 pp.

[25] J. Sullivan, "Boundary lubrication and oxidational wear," Journal of Physics D: Applied Physics, 19(10) (1986), 1999-2011 pp.